Transport and Localization of Exogenous Myelin Basic Protein mRNA Microinjected into Oligodendrocytes

Kevin Ainger,* Daniela Avossa,* Frank Morgan,* Sandra J. Hill,‡ Christopher Barry,‡ Elisa Barbarese,‡ and John H. Carson*

*Departments of Biochemistry and ‡Neurology, University of Connecticut Health Center, Farmington, Connecticut 06030

Abstract. We have studied transport and localization of MBP mRNA in oligodendrocytes in culture by microinjecting labeled mRNA into living cells and analyzing the intracellular distribution of the injected RNA by confocal microscopy. Injected mRNA initially appears dispersed in the perikaryon. Within minutes, the RNA forms granules which, in the case of MBP mRNA, are transported down the processes to the periphery of the cell where the distribution again becomes dispersed. In situ hybridization shows that endogenous MBP mRNA in oligodendrocytes also appears as granules in the perikaryon and processes and dispersed in the peripheral membranes. The granules are not released by extraction with non-ionic detergent, indicating that they are associated with the cytoskeletal matrix. Three dimensional visualization indicates that MBP mRNA granules are often aligned in tracks along microtubules traversing the cytoplasm and processes. Several distinct patterns of granule movement are observed. Granules in the processes undergo sustained directional movement with a velocity of ~0.2 μm/s. Granules at branch points undergo oscillatory motion with a mean displacement of 0.1 μm/s. Granules in the periphery of the cell circulate randomly with a mean displacement of ~1 μm/s. The results are discussed in terms of a multi-step pathway for transport and localization of MBP mRNA in oligodendrocytes. This work represents the first characterization of intracellular movement of mRNA in living cells, and the first description of the role of RNA granules in transport and localization of mRNA in cells.

In eukaryotic cells certain mRNAs are spatially restricted to discrete regions within the cell. The most general example is the localization of mRNAs for secretory and membrane proteins to the rough ER, which is mediated by a signal sequence in the nascent polypeptide chain (Pfeffer and Rothman, 1987). Other specific examples of localized mRNAs have been demonstrated in very large cells such as Xenopus oocytes or Drosophila embryos, in very flat cells such as mammalian cells in tissue culture, and in cells with very polarized morphologies such as neurons and glia of the central nervous system (CNS).[1]

In Xenopus oocytes, the large size of the cell facilitates physical dissection of the animal and vegetal poles. This technique has been used to demonstrate that some mRNAs (Vg1) are localized to the vegetal pole, while other mRNAs (An2) are localized to the animal pole (Rebagliati et al., 1985). In Drosophila embryos, in situ hybridization has been used to demonstrate localization of certain maternal transcripts during oogenesis and embryogenesis. The maternal transcript of the bicoid gene is synthesized in nurse cells, and then transported into the oocyte, where it is localized to the anterior pole (Berleth et al., 1988). During oogenesis, nanos, tudor, and oskar mRNAs are localized to the posterior pole of the developing oocyte (Ephrussi et al., 1991; Golumbeski et al., 1991; Kim-Ha et al., 1991; Wang and Lehmann, 1991). Later in Drosophila development, mRNAs for even-skipped, fushi tarazu, hairy, and runt are localized to the peripheral cytoplasm of the syncitial blastoderm (Ingham et al., 1985; Weir and Kornberg, 1985; Macdonald et al., 1986; Gergen and Butler, 1988).

In situ hybridization has also been used to demonstrate localization of specific mRNAs in cultured mammalian cells. Cells spreading on a substratum localize actin mRNA to the lamellipodia (Singer et al., 1989). Messenger RNAs for other cytoskeletal components (tubulin and vimentin) are also localized to discrete regions of the cell (Lawrence and Singer, 1986). Other mRNAs reported to be localized in mammalian cells are protamine 1 (Braun et al., 1989) and the nicotinic acetyl choline receptor alpha-subunit (Fontaine et al., 1988).

In the mammalian CNS, many cell types send out long processes from the cell body, or perikaryon. In particular anatomical sites, such as the hippocampus, the cell bodies

Please address all correspondence to Dr. John H. Carson, Department of Biochemistry, University of Connecticut Health Center, Farmington, CT 06030.

1. *Abbreviations used in this paper*: CNS, central nervous system; CSK, cytoskeleton; DEPC, diethylpyrocarbonate; FTSC, fluorescein thiosemicarbazide; MBP, myelin basic protein.

and processes occupy distinct strata. This anatomical separation of cell body and processes has allowed the use of in situ hybridization in CNS sections to study the subcellular localization of specific mRNAs in neurons. In this way, microtubule-associated protein 2 (Bruckenstein et al., 1990; Kleiman et al., 1990) and the alpha subunit of calcium/calmodulin-dependent protein kinase (Burgin et al., 1990) mRNAs have been shown to be localized to dendrites and excluded from axons. Conversely, oxytocin and vasopressin mRNAs are localized to axons, but not dendrites (Mohr et al., 1991).

In oligodendrocytes, which send out as many as 50 processes which wrap around axons and form the myelin sheaths in the CNS, myelin basic protein (MBP) mRNA is localized to the distal processes. This has been demonstrated both by in situ hybridization in intact tissue (Kristensson et al., 1986; Verity and Campagnoni, 1988), and by subcellular fractionation of myelin membranes from the brain (Colman et al., 1982). MBP mRNA has also been shown to be localized to the cell periphery in cultured oligodendrocytes by in situ hybridization (Holmes et al., 1988; Shiota et al., 1989; Barbarese, 1991).

The phenomenon of mRNA localization is clearly established in a variety of systems. However, little is known about the mechanism by which localization is achieved. Drugs which disrupt microtubules and microfilaments perturb the establishment and the stabilization, respectively, of Vgl mRNA localization in the Xenopus oocyte (Yisraeli et al., 1990). In mammalian cells disruption of actin filaments prevents actin mRNA localization, while disruption of microtubules has no effect (Sundell and Singer, 1991). These studies suggest that the cytoskeleton is involved in mRNA localization.

Most of the previous work on mRNA localization has focused on the steady state distribution of total endogenous mRNA in fixed cells. This is an equilibrium condition and may not be directly relevant to understanding the mechanism of RNA localization, which is a dynamic process. Analysis of the dynamics and kinetics of mRNA movement in living cells is needed to answer fundamental questions about the localization mechanism.

Towards this end, we have studied the intracellular distribution and movement of exogenous MBP mRNA microinjected into mouse oligodendrocytes growing in primary culture. These cells have a characteristic morphology which is particularly advantageous for these studies. First, the cell body is small and rounded and protrudes from the substrate, providing an excellent target for microinjection. Second, the processes and peripheral membranes are extremely thin and flat, providing excellent optical properties for microscopy. This makes it possible to study the three dimensional process of intracellular transport in an essentially two dimensional system. These morphological peculiarities notwithstanding, the oligodendrocyte in culture recapitulates many of the salient features of myelin morphogenesis in vivo, and thus provides a good experimental system in which to analyze the dynamics of MBP mRNA transport and localization.

Materials and Methods

Cell Culture

Mouse oligodendrocytes were isolated from mixed primary brain cell cultures after 12–14 d of growth, as described by Barbarese (1991). The enriched cell population was grown in a mixture of defined medium (Bottenstein, 1986) and conditioned medium from the mouse neuronal cell line C1300 in a 2:1 ratio (Giulian et al., 1991). Cells were allowed to differentiate for 2–3 d after plating before the start of experiments. NIE-115 mouse neuroblastoma cells (Kimhi et al., 1976) were obtained from Dr. Leslie Loew (University of Connecticut Health Center, Farmington, CT) and were grown in 10% newborn calf serum in DME. Before microinjection, NIE-115 cells were plated sparsely on coverslips and treated with differentiation medium containing 0.5% newborn calf serum, 1% DMSO in DME, for 3 d, to induce process outgrowth.

Reagents

Restriction enzymes and RNA polymerases were obtained from New England BioLabs (Beverly, MA), Promega (Madison, WI), and Stratagene (La Jolla, CA). RNasin and transcription buffers were from Promega. RNA molecular weight markers were obtained from GIBCO BRL (Gaithersburg, MD). Diethylpyrocarbonate (DEPC), mineral oil, and ammonium sulfate were from Sigma Chem. Co. (St. Louis, MO).

Recombinant DNA

Full length cDNA for rat 14 kD MBP was reconstructed from pMBP-1 and pMBP-3 (obtained from Dr. A. Roach and described in Roach et al., 1983). The reconstructed MBP cDNA was subcloned into pBluescript II (Stratagene) which contains T3 and T7 promoters. pSP64-Xβm, containing a full length cDNA from *Xenopus laevis* β-globin, cloned in an SP6 vector, was obtained from Dr. D. Melton (Harvard, Cambridge, MA). Full length cDNA for mouse β-actin, cloned in Bluescript was obtained from Dr. J. Pachter (University of Connecticut Health Center, Farmington, CT).

Transcription and RNA Labeling

RNA for microinjection was synthesized in vitro from full length cDNA clones to generate MBP mRNA and, as controls, globin and actin mRNAs. To analyze intracellular distribution and movement, injected RNA was labeled with a reporter moiety to enable visualization. We used two different protocols to label RNA. In one protocol, a single fluorophore was covalently conjugated to the 3′ end of the RNA. This provides a stoichiometric label on each RNA molecule, which should not affect translation, and which can be visualized directly in living cells. However, the fluorescent label is potentially subject to photobleaching and photodamage during microscopic imaging, which may degrade the image quality and interfere with accurate determination of intracellular distribution. In the second protocol, digoxigenin-labeled ribonucleotides were incorporated into the body of the mRNA during synthesis. The digoxigenin-labeled RNA was visualized using anti-digoxigenin antibodies. This provides a greatly amplified signal with improved image quality. However, the digoxigenin moiety may inhibit translation of the RNA, and the cells must be fixed before antibody labeling, either of which could affect the intracellular distribution. The use of these two different labeling protocols provides important controls for potential effects of the image reporter or the imaging procedure on RNA localization.

Digoxigenin-labeled RNA was prepared by in vitro transcription using Promega buffers and protocols. Digoxigenin-11-rUTP was obtained from Boehringer Mannheim (Indianapolis, IN) and was used as recommended by the manufacturer. Under these conditions digoxigenin-modified ribonucleotides are incorporated every 30–40 residues. Transcription reactions were treated with RNase-free DNase and precipitated with potassium acetate and ethanol. All samples were dissolved in water and filtered through 0.22 μm spin filters (Millipore, Bedford, MA) before microinjection. Transcription products were analyzed by agarose gel electrophoresis with RNA markers to determine transcript length and to monitor degradation. Only full-length, nondegraded samples were used for microinjection.

Fluorescein-labeled RNA was prepared by a modification of the method of Wells and Cantor (1977, 1980). RNA was transcribed with unsubstituted ribonucleotides, treated with RNase-free DNase, extracted with phenol:chloroform and chloroform, and ethanol precipitated. The RNA (5–500 μg) was dissolved in 58.7 μl DEPC-treated water, and sodium acetate was added to a final concentration of 0.1 M, pH 5. One tenth volume of 500 mM sodium m-periodate at 37°C was added and the RNA was incubated at 37°C, for 30 min, in the dark. Ethylene glycol (2 μl) was added, and the sample was incubated at room temperature, for 5 min. The final sample volume of 70 μl was gel filtered through a push column (Nuctrap, Stratagene) in 0.1 M sodium acetate, pH 5, and extracted with phenol:chloroform and chloroform. Fluorescein thiosemicarbizide (FTSC) (Molecular Probes, Eugene, OR) was added to at least a 25 molar excess over RNA 3′ ends and

the sample was incubated at 37°C, for 30 min, in the dark. The fluorescein-conjugated RNA was extracted with phenol:chloroform and chloroform, and ethanol precipitated to remove most of the unconjugated FTSC. The RNA was gel filtered to remove any residual FTSC, extracted with phenol:chloroform and chloroform, and ethanol precipitated. The fluorescein-conjugated RNA was analyzed by agarose gel electrophoresis. No unincorporated FTSC was detected. The coupling efficiency was determined to be >90%, using a Spex Fluorolog fluorometer (Spex Industries, Edison, NJ) with FITC (Molecular Probes) in 10 mM Tris-HCl, pH 8.0, as a standard.

Microinjection and Immunocytochemistry

Before injection, cells were rinsed with Hepes buffered Dulbecco's PBS (GIBCO BRL). Cells were microinjected at room temperature in Dulbecco's PBS. RNA concentrations were 0.5–1.0 mg/ml in water. Cells injected with digoxigenin-RNA were incubated at 37°C, for 10 min, to allow time for RNA transport. Cells were fixed with 4% paraformaldehyde in 5 mM $MgCl_2$, PBS for 30 min, washed with PBS, and stored at 4°C.

Immunocytochemistry followed manufacturer recommendations for in situ hybridization, with the following changes. Nonspecific binding was blocked using 0.5% Boehringer Mannheim Blocking Reagent, and 10% normal goat serum, in 100 mM Tris-HCl, 150 mM sodium chloride, pH 7.5. Blocking reagent and serum were treated to inactivate nucleases by incubating (5 mg/ml protein in 100 mM potassium phosphate, pH 7.4) with 5 mM acetic anhydride. This was repeated 10 times while maintaining neutral pH. Proteins were precipitated with ammonium sulfate, and dialyzed against 100 mM Tris-HCl, 150 mM sodium chloride, pH 7.5. Nuclease activity was assayed by incubation with RNA molecular weight markers, followed by agarose gel electrophoresis. Alkaline phosphatase–conjugated polyclonal Fab anti-digoxigenin was used at 1:1,000 dilution. Vector Red (Vector Lab, Burlingame, CA) was used according to manufacturer suggestions. Coverslips were dehydrated in 70, 95, and 100% ethanol, Histo-Clear (National Diagnostics, Atlanta, GA), and mounted in Permount (Fisher Scientific, Fair Lawn, NJ).

Labeling for tubulin was performed on fixed cells after permeabilization with detergent. Rabbit anti-tubulin (Accurate, Westbury, NY) was used at a 1:100 final dilution. Fluorescein-conjugated goat anti–rabbit antibody was obtained from Organon-Teknica, and used at 1:100 final dilution.

Fluorescent RNA was injected into cells on a coverslip suspended between supports in a plastic petri dish, in a Leiden environmental microchamber (Medical Systems Corp., Greenvale, NY), on the stage of an upright confocal microscope. The petri dish was filled with Dulbecco's PBS. RNA was injected underneath the coverslip with a flame-bent microinjection needle pulled on a Flaming Brown Micropipette Puller (Sutter Instruments, San Rafael, CA). Flame-bent needles were prefilled with 1 μl nuclease-free mineral oil before loading with RNA.

Glass capillaries were treated overnight with 3.5% (vol/vol) saturated potassium dichromate in concentrated sulfuric acid and washed extensively with filtered DEPC-water to minimize dust and nuclease contamination.

Cell Extraction

This protocol is essentially that of Biegel and Pachter (1991), with minor modifications. The cells were first washed with PBS followed by cytoskeleton (CSK) buffer (0.3 M sucrose, 0.001 M EGTA, 0.01 M Pipes, pH 6.8, 0.025 M KCL, 0.005 M $MgCl_2$). The cells were then treated with the extraction buffer (CSK buffer containing 0.2% Triton X-100) at room temperature for 30–40 s, and rinsed sequentially with CSK buffer and PBS. The remaining "extracted" cells were fixed at room temperature, for 20 min in 4% phosphate-buffered paraformaldehyde.

In situ Hybridization

In situ hybridization was performed according to the protocol of Singer et al. (1986) with minor modifications. The procedure was carried out shortly after fixation of the cells with paraformaldehyde as described above. The samples were never stored in alcohol. Digoxigenin-labeled probe for in situ hybridization was prepared by the random oligonucleotide priming method (Feinberg and Vogelstein, 1983) (overnight, 37°C) according to the manufacturer instructions (Boehringer Mannheim) using dUTP-digoxigenin. The DNA template was a 1.5-kb EcoRI insert fragment representing a partial cDNA for rat 14K MBP (Roach et al., 1983) cloned into a Bluescript II vector (Stratagene). After hybridization, the cells were fixed again, and rinsed with PBS, and with 0.2 M Tris-HCl, pH 7.4, 0.1 M glycine for 10 min. The cells were treated with 0.1% NP-40 in PBS for 5 min, and incubated with 5% BSA in PBS for 15 min. Immunocytochemistry was performed using a mouse mAb to digoxigenin (1:50, Boehringer Mannheim) (2 h at room temperature), and fluorescein- or Texas red–conjugated goat anti–mouse antibodies (1:50, Organon Teknica; 1 h at room temperature). The cells were rinsed with PBS and mounted in a 3% solution of 1,4-diazabicyclo[2.2.2.]octane in glycerol.

Microscopy and Image Processing

Laser scanning confocal microscopy was performed with an MRC-600 scanning system (Biorad, Cambridge, MA) mounted on an Axioskope (Zeiss, Oberkochen, Germany) equipped with a variety of infinity-corrected high numerical aperture objectives. Time lapse confocal image collection

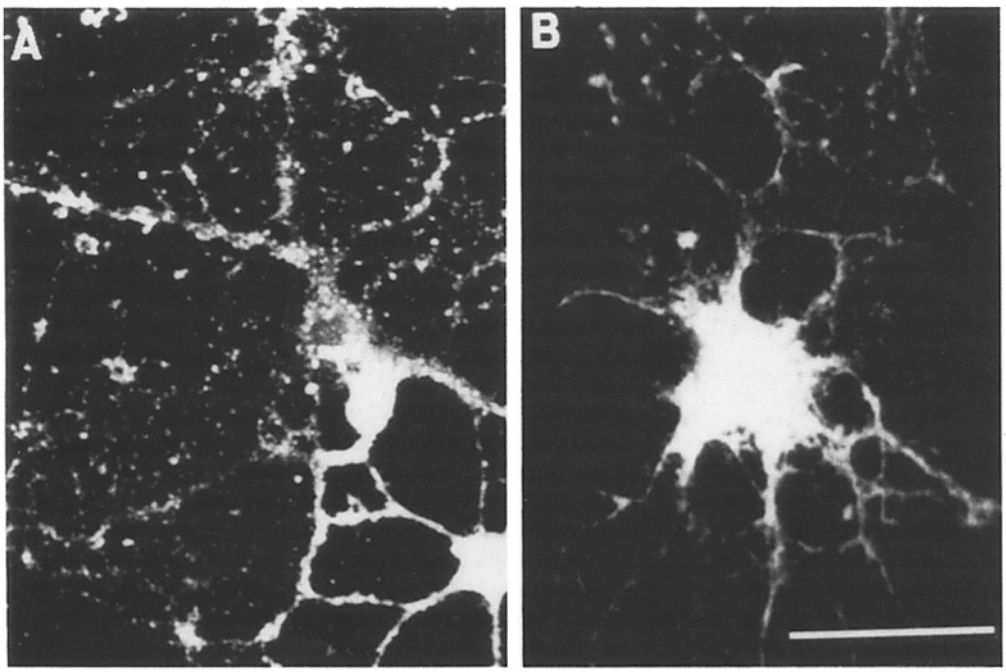

Figure 1. Digoxigenin-labeled exogenous MBP mRNA microinjected into oligodendrocytes: before and after CSK extraction. Digoxigenin-labeled MBP mRNA was microinjected into mouse oligodendrocytes as described in Materials and Methods. The cells were rinsed with PBS (*A*), or treated with CSK extraction buffer (*B*). Digoxigenin-labeled RNA was visualized by immunocytochemistry and confocal laser scanning microscopy. The two cells shown are representative of several thousand injected cells that were examined. Bar, 25 μm.

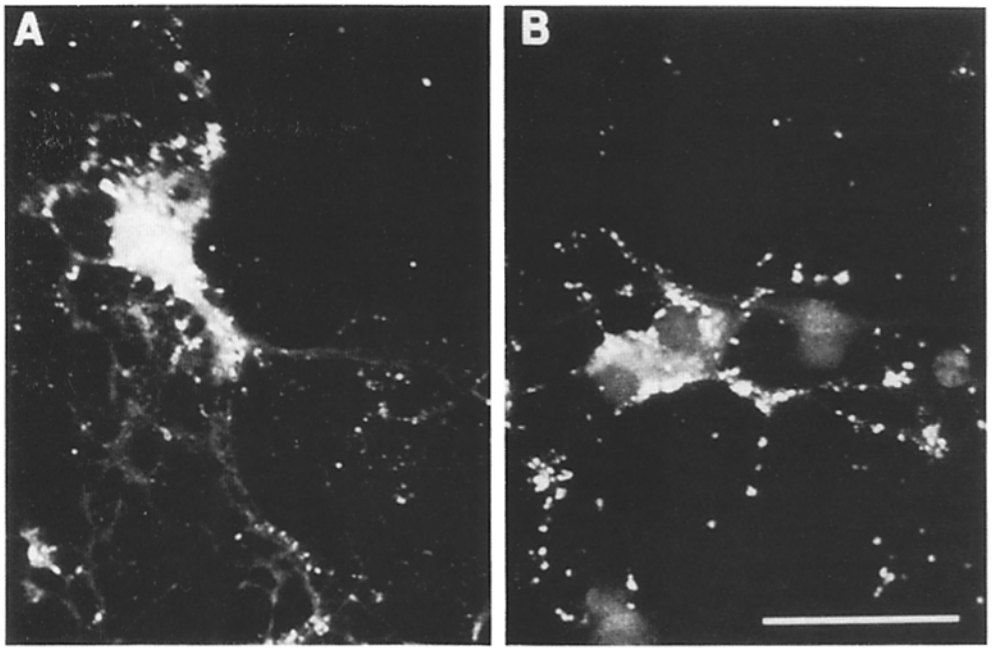

Figure 2. In situ hybridization of endogenous MBP mRNA in oligodendrocytes before and after CSK extraction. Oligodendrocytes grown in culture were rinsed with PBS (*A*), or treated with CSK extraction buffer (*B*). Control and treated cells were fixed, processed for in situ hybridization, and immunostained with anti-digoxigenin as described in Materials and Methods. Bar, 50 μm.

was controlled by a specialized command file written for this purpose. Series of optical sections for three dimensional reconstruction were collected at 0.5 μm intervals. This approximates the optical resolution in the z axis of the microscope with the objective used (60×, 1.4 NA). Three dimensional image data was reconstructed and visualized using an SGI Iris 340 VGX graphics supercomputer (Silicon Graphics, Inc., Mountain View, CA). Volume visualization was performed using Voxelview (Vital Images, Fairfield, IA). Isosurface visualization was performed using a marching cubes algorithm described previously (Morgan et al., 1992).

Results

Microinjected MBP mRNA Forms Intracellular Granules

To analyze the intracellular distribution of exogenous RNA, digoxigenin-labeled MBP RNA was microinjected into mouse oligodendrocytes growing in primary culture (Fig. 1 *A*). The injected RNA appeared as small granules which were present throughout the cytoplasm and processes, and was also found dispersed in the peripheral membranes of the cell. The granules were relatively uniform in size (~0.3 μm in diameter) and intensity. Most cells contained several hundred granules but the number varied with the amount of RNA injected. Granule formation was not due to the reporter molecule incorporated into the RNA or to the procedure used for visualization, because fluorescein-labeled MBP mRNA formed similar granules when microinjected into oligodendrocytes and visualized directly in living cells (see Fig. 6 *A–F*).

Endogenous MBP mRNA in Oligodendrocytes Is Also Present in Granules

The distribution of endogenous MBP mRNA in oligodendrocytes was examined by high resolution fluorescent in situ hybridization (Fig. 2 *A*). MBP mRNA appeared as granules in the perikaryon and processes and dispersed in the peripheral membranes of the cell. Control experiments where the primary antibody was omitted or where shiverer oligodendrocytes (which contain no endogenous MBP because of a deletion in the MBP gene) were used, showed no granules and no dispersed staining in the periphery of the cell (data not shown). The number of endogenous MBP mRNA granules per cell was generally less than the number of exogenous RNA granules in injected cells. However the size and intracellular distribution of the endogenous RNA granules was similar to the exogenous RNA granules. Since the intracellular distributions of both endogenous and exogenous MBP mRNA in oligodendrocytes are similar, it is likely that this accurately reflects the intracellular distribution of MBP mRNA in oligodendrocytes.

Endogenous and Exogenous MBP mRNA Granules Are Associated with the Cytoskeletal Matrix

Both endogenous and exogenous MBP mRNA granules sometimes appeared to be aligned in tracks traversing the cytoplasm and processes, suggesting that they were associated with the cytoskeleton. To test this possibility, cells were extracted with non-ionic detergent which dissolves the cell membrane, releasing soluble cytoplasmic components and leaving the cytoskeletal matrix intact. Both exogenous (Fig. 1 *B*) and endogenous (Fig. 2 *B*) MBP mRNA granules remained associated with the cytoskeletal matrix after detergent extraction. In the case of endogenous MBP mRNA, dispersed RNA in the perikaryon was extracted. In the case of exogenous MBP mRNA, the concentration of granules obscured the dispersed RNA in the perikaryon so it was difficult to determine if it was extracted. In both cases the dispersed RNA in the peripheral membranes was extracted. These results indicate that both exogenous and endogenous MBP mRNA granules are associated with the oligodendrocyte cytoskeleton, while dispersed MBP mRNA is not. Cytoskeletal components in oligodendrocytes include microtubules and microfilaments but not intermediate filaments (Kachar et

al., 1986). Thus, it is likely that the MBP mRNA granules are associated with either microtubules or microfilaments.

Three Dimensional Visualization of MBP mRNA Granules in Oligodendrocytes

The images in Figs. 1 and 2 represent individual confocal optical sections through the cell. In each case the focal plane was immediately adjacent to the coverslip in order to visualize the flat processes and peripheral membrane sheets elaborated by the oligodendrocyte. Because of the thickness of the cell body, some of the RNA in the cell was not included in the optical section, and does not appear in these images. To analyze the three dimensional distribution of microinjected labeled MBP mRNA throughout the cell, consecutive optical sections through a single oligodendrocyte were collected, reconstructed, and visualized using volume rendering (Fig. 3 *A*) or isosurface rendering (Fig. 3 *B*) techniques.

An oligodendrocyte microinjected with MBP mRNA, visualized by volume rendering is shown in Fig. 3 *A*. RNA granules were observed throughout the perikaryon and in some, but not all, processes. The granules in the perikaryon and in the processes appeared to be equivalent in size. In some regions the granules in the processes were aligned in tracks. Although not apparent from this image, the nucleus was devoid of granules.

A small subvolume of an oligodendrocyte in which both injected MBP mRNA and endogenous tubulin were imaged simultaneously, visualized by isosurface rendering is shown in Fig. 3 *B*. In this image the isosurface corresponding to the surface of the process was rendered with partial transparency to reveal the surfaces of a microtubule bundle (green) and of several RNA granules (red) within the process. The granules appeared relatively uniform in size although they displayed a variety of different shapes. Their exact dimensions are uncertain because they are close to the resolution limits of the microscope and because they may contain other components in addition to the labeled RNA which was visualized. The RNA granules appeared to be closely apposed to the microtubule bundle in the center of the process. This does not necessarily imply direct interaction between RNA and microtubules since both the RNA granules and the microtubule bundle are confined within the small volume of the process. Nevertheless, the RNA granules do appear to be closely associated with the microtubule bundle and may be transported along it. Similar colocalization studies using in situ hybridization and immunocytochemistry indicate that endogenous MBP mRNA granules are also aligned along microtubules in oligodendrocytes (Barbarese, unpublished data).

MBP mRNA Is Differentially Transported to the Periphery in Oligodendrocytes

The spatial distribution of mRNA within the cell was strikingly dependent on the type of mRNA injected. In the case of MBP mRNA (Figs. 1 *A* and 4 *A*), granules were observed in the perikaryon, throughout the length of the processes, and in the expanses of membrane sheets elaborated by oligodendrocytes. In addition, MBP mRNA also appeared dispersed in the peripheral membrane sheets. In the case of globin mRNA (Fig. 4 *B*), granules were formed but remained in the perikaryon, and were not observed in the processes and membrane sheets, and globin mRNA never appeared dispersed in the membrane sheets. Actin mRNA also formed granules which showed a distribution similar to that of globin mRNA (data not shown). However, fluorescein-labeled tRNA and fluorescein-conjugated dextran both remained disperse in the perikaryon and did not form granules (data not shown). This indicates that granule formation is a property of mRNAs in general, but not of other RNAs or polysaccharides. Moreover, transport of RNA granules down the processes to the periphery of the oligodendrocyte is specific for MBP mRNA.

Formation of mRNA Granules and Differential Transport of MBP mRNA Granules to the Cell Periphery Is Also Observed in Neuroblastoma Cells

Formation of RNA granules and differential transport of MBP mRNA granules to the cell periphery presumably requires specific factors and transport machinery within the cell. To test whether these factors and machinery were present in other cells, MBP and globin mRNAs were injected into NIE-115 neuroblastoma cells (Fig. 5, *A* and *B*). These cells extend long neurites but do not elaborate large flat membrane sheets like oligodendrocytes. Both MBP mRNA and globin mRNA formed granules in NIE-115 cells. The MBP mRNA granules were transported down the processes while globin mRNA granules remained in the perikaryon. These results indicate that the factors necessary for formation of RNA granules and the cellular machinery necessary for differential transport of MBP mRNA granules to the periphery of the cell are not specific to oligodendrocytes, but are also present in other cells with extended processes.

Time Lapse Analysis of MBP mRNA Granule Formation in Oligodendrocytes

To analyze the dynamics of RNA granule formation, fluorescein-labeled MBP mRNA was microinjected into oligodendrocytes, and series of sequential images were collected at different time points. One example is shown in Fig. 6, *A–F*. Immediately after injection, fluorescent RNA is dispersed uniformly throughout the perikaryon. Within minutes, the fluorescence in the perikaryon begins to appear granular. By 7 min after injection, most of the fluorescence is present in discrete granules which are visible throughout the perikaryon and processes. In some regions the granules are aligned in tracks which traverse the cytoplasm and continue into the processes. Eventually, fluorescent RNA accumulates in a disperse pattern in flat membranous regions in the periphery of the cell. In the cell in Fig. 6, disperse fluorescence is visible in flat membranes immediately adjacent the perikaryon on the left. This cell is somewhat atypical in that granule formation was relatively prolonged. In many cells granule formation occurred within the first minute after injection at room temperature and even more rapidly at 37°C. When mRNA was injected into the nucleus, it did not form granules and did not leave the nucleus (data not shown). These results indicate that MBP mRNA forms granules soon after it appears in the cytoplasm and that the granules are rapidly transported to the periphery of the cell.

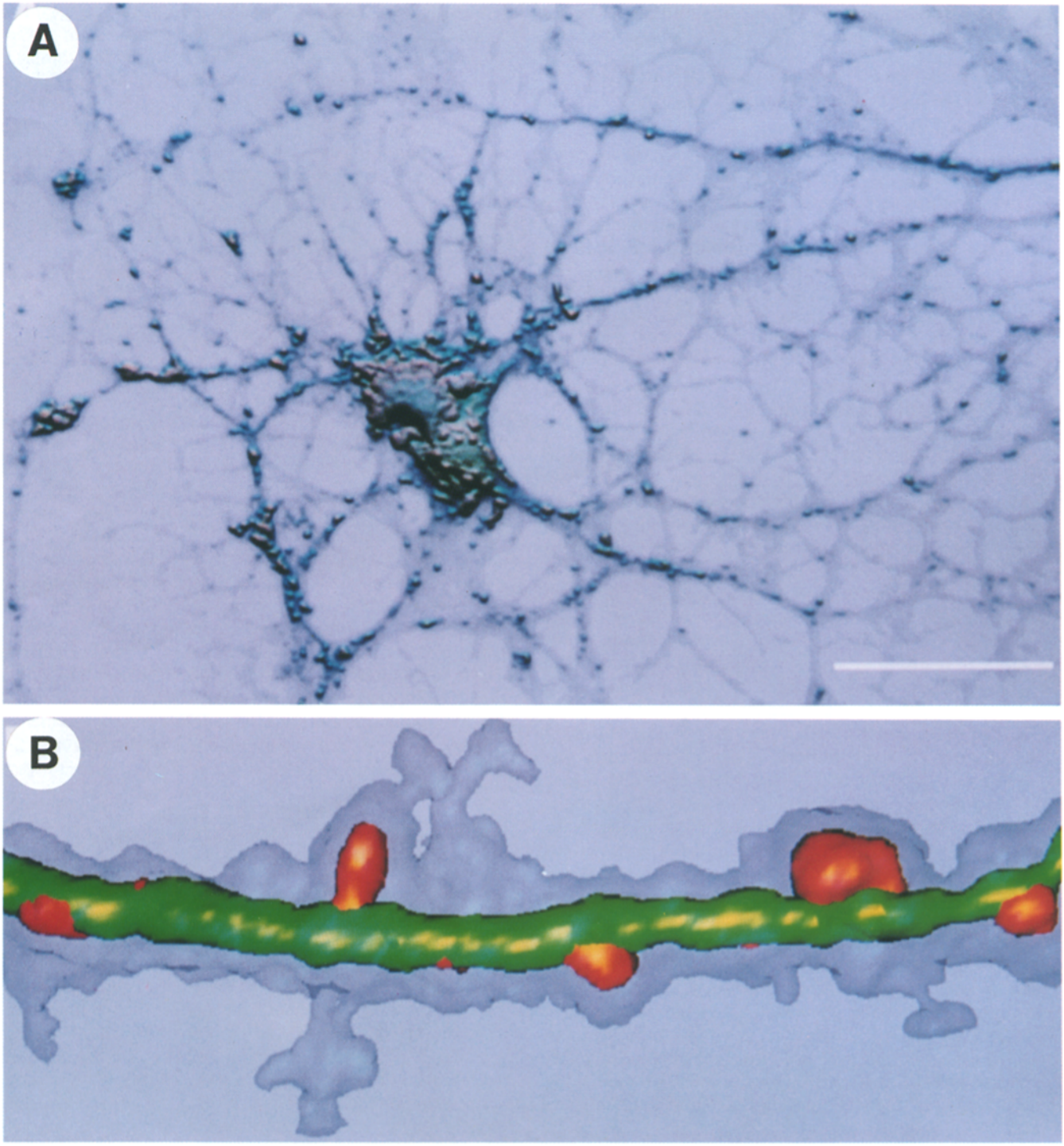

Figure 3. Three dimensional visualization of digoxigenin-labeled MBP mRNA microinjected into oligodendrocytes. Digoxigenin-labeled MBP mRNA was microinjected into mouse oligodendrocytes and visualized as described in Fig. 1 *A*. A series of 20 optical sections was collected at 0.5-μm intervals through the cell. The data was reconstructed in three dimensions and displayed using volume rendering (*A*). Voxels were rendered with an opacity gradient corresponding to the gray scale values except that low level fluorescence corresponding to nonspecific staining of the cytoplasm was displayed with slightly enhanced opacity to delineate the cell volume. High level fluorescence corresponding to digoxigenin-labeled RNA was displayed with specular highlighting to accentuate the RNA granules. The scale bar in *A* corresponds to 25 μm. *B* shows isosurface rendering of subvolume containing a portion of an oligodendrocyte process from a cell immunostained simultaneously for both injected MBP mRNA and tubulin. An isosurface boundary of 15 was calculated to delineate the volume occupied by low level, nonspecific fluorescence in the oligodendrocyte process. This isosurface is rendered with partial transparency to reveal surfaces within the process. An isosurface boundary of 59 in the green channel was calculated to delineate the surface of a microtubule bundle contained in the process. This surface is shown in green. An isosurface boundary of 150 in the red channel was calculated to delineate the volume occupied by high level fluorescence in RNA granules. This isosurface is shown in red. The different isosurfaces are rendered with Gouraud shading and specular highlighting. A scale bar is not included in *B* because of perspective effects within the image.

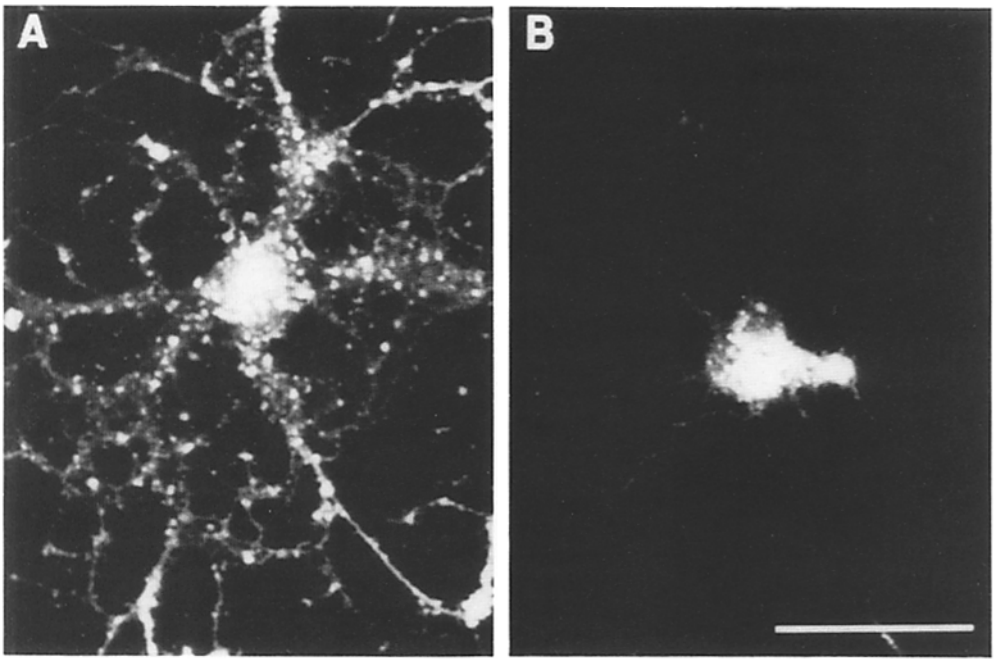

Figure 4. Digoxigenin-labeled MBP mRNA and globin mRNA microinjected into oligodendrocytes. Digoxigenin-labeled MBP mRNA (*A*) and globin mRNA (*B*) were microinjected into mouse oligodendrocytes as described in Materials and Methods. The digoxigenin-labeled RNA was visualized by immunocytochemistry and confocal laser scanning microscopy. The two cells shown are representative of several thousand injected cells that were examined. Bar, 25 μm.

Time Lapse Motion Analysis of MBP mRNA Granules in Oligodendrocytes

To analyze motion of MBP mRNA granules in oligodendrocytes, series of confocal images were collected at sequential time points. In most cells, the majority of granules were relatively immobile. To identify mobile granules, each series of time lapse images was displayed as an animation loop with time compression. Granules which exhibited significant displacements (>1 μm) relative to immobile fiduciary features of the cell over the course of the time series were classified as mobile.

Granules in oligodendrocyte processes displayed two types of motion. Fig. 7 shows a series of images from a portion of an oligodendrocyte process containing a single mobile granule. The granule moved continuously down the process for ~60 s with a sustained velocity of ~0.2 μm/s. When it reached a branch point, continuous motion was interrupted, and the granule underwent oscillatory motion for ~60 s, with a mean displacement of ~0.1 μm/s. By direct observation using epifluorescence microscopy, mobile granules were observed to move continuously in oligodendrocyte processes for distances greater than 50 μm, sometimes

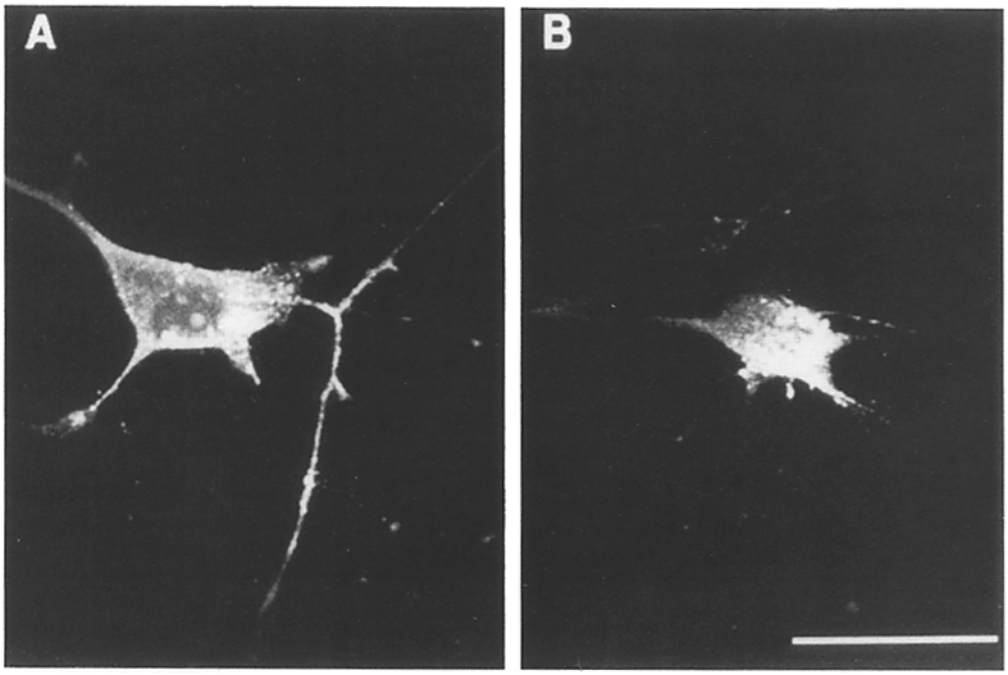

Figure 5. Digoxigenin-labeled MBP mRNA and globin mRNA microinjected into NIE-115 neuroblastoma cells. Digoxigenin-labeled MBP mRNA (*A*) and globin mNRA (*B*) were microinjected into NIE-115 neuroblastoma cells as described in Materials and Methods. The digoxigenin-labeled RNA was visualized by immunocytochemistry and confocal laser scanning microscopy. Bar, 50 μm.

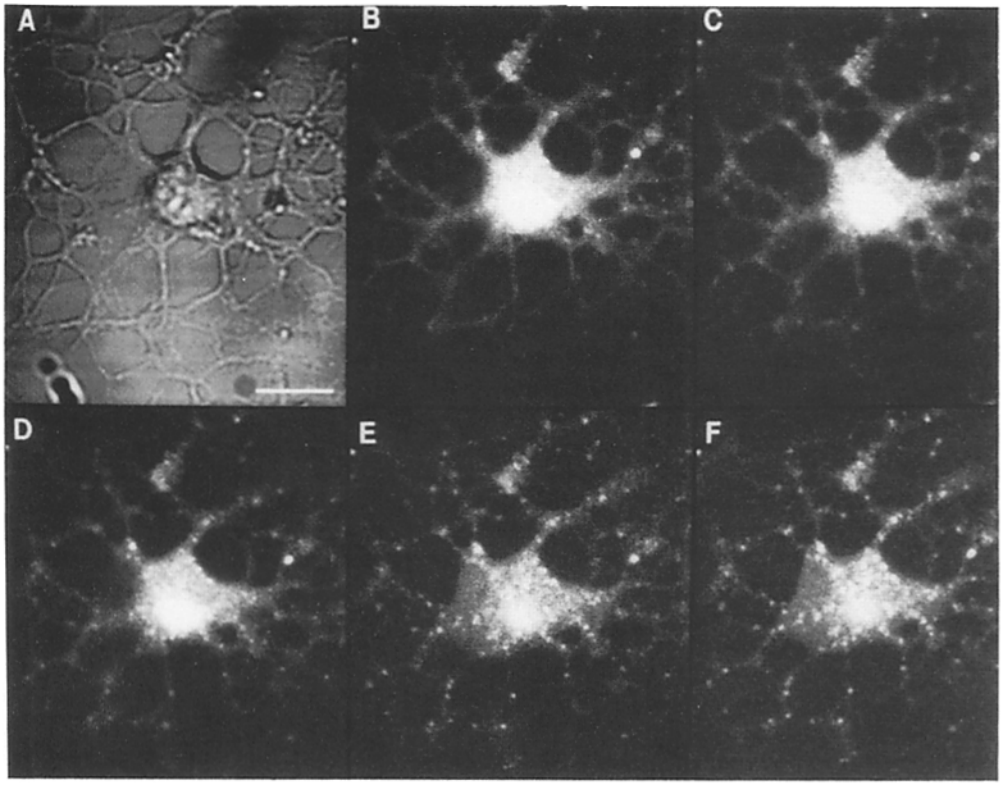

Figure 6. Time lapse analysis of RNA granule formation in oligodendrocytes. Fluorescein-labeled MBP mRNA was microinjected into an oligodendrocyte as described in Materials and Methods. A series of sequential confocal microscopic images were collected at different times after injection. (*A*) Scanning transmitted light image of the cell before injection, Bar, 10 μm; (*B*) scanning confocal fluorescent image immediately (less than 10 s) after injection; (*C*) 100 s after injection; (*D*) 200 s after injection; (*E*) 440 s after injection; (*F*) 660 s after injection.

negotiating branch points without interruption. The direction of granule movement was always anterograde from the perikaryon to the periphery of the cell. Retrograde movement of granules from the periphery towards the perikaryon was never observed.

Granules in the peripheral membranes displayed a third type of motion. Fig. 8 shows a series of images from a portion of oligodendrocyte peripheral membrane containing several mobile granules. These granules circulate randomly and independently with mean displacements of ~1 μm/s. Cumulative trajectories for three different granules are traced in the last panel. Conclusions concerning the mechanisms of granule mobility will require comprehensive motion analysis involving systematic and extensive measurements on large numbers of granules.

Discussion

The work described in this paper was undertaken to elucidate the mechanisms for transport and localization of MBP mRNA in oligodendrocytes. The results describe the intracellular distribution of exogenous MBP mRNA microinjected into oligodendrocytes in culture. Microinjected MBP RNA forms intracellular granules in the perikaryon which are transported to the processes and peripheral membranes. Eventually the RNA appears dispersed in the peripheral membranes of the cell. We propose that the various forms in which the injected RNA appears represent intermediates in a linear multistep transport pathway leading to localization of MBP mRNA in the peripheral processes and membranes of oligodendrocytes. The pathway is diagrammed in Fig. 9.

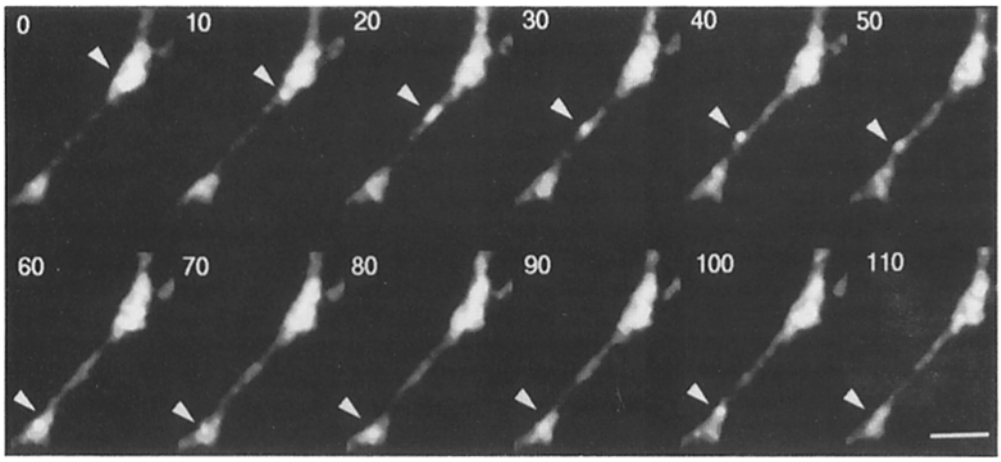

Figure 7. Time lapse analysis of RNA granule motion in an oligodendrocyte process. Fluorescein-labeled MBP mRNA was microinjected into an oligodendrocyte as described in Materials and Methods. A series of sequential confocal microscopic images were collected at 10-s intervals. A small portion of an oligodendrocyte process containing a mobile granule is shown. The position of the granule within the process is indicated by an arrowhead. Bar, 5 μm.

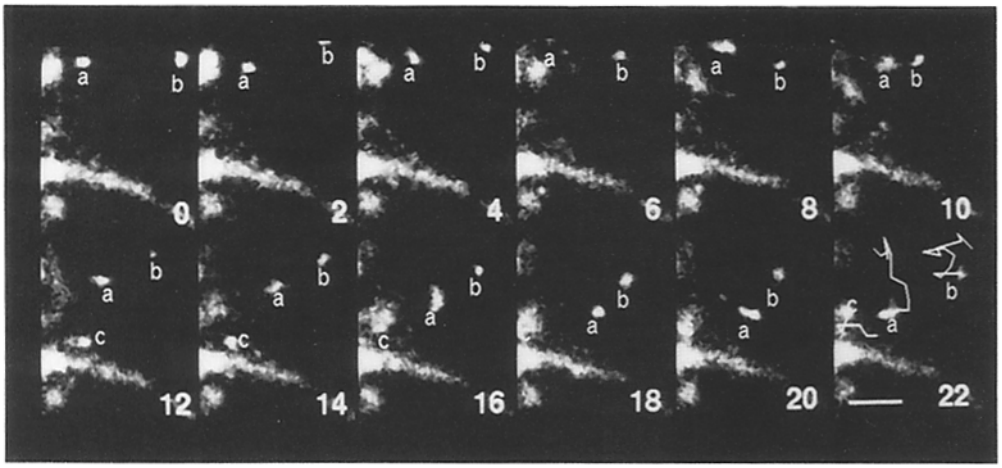

Figure 8. Time lapse analysis of RNA granule motion in oligodendrocyte membranes. Fluorescein-labeled MBP mRNA was microinjected into an oligodendrocyte as described in Materials and Methods. A series of sequential confocal microscopic images were collected at 2-s intervals. A small portion of oligodendrocyte membrane containing several mobile granules is shown. The positions of three separate granules within the membrane are indicated by *a*, *b*, and *c*. In some frames individual granules appear elongated or non-spherical. This is because the motion of the granule is significant in relation to the scan time of the microscope. The sequential positions of the approximate centroids of each of the three granules are shown as cumulative trajectories in the last frame. Bar, 10 μm.

The proposed pathway is based on the assumption that each of the observed intermediates is involved with transport and localization of MBP mRNA in oligodendrocytes. It is possible that some of the intermediates are involved in other aspects of RNA metabolism, such as translation or degradation. These alternatives cannot be evaluated based on the data presented here and will not be discussed further.

The proposed pathway is inferred from observations of both exogenous and endogenous MBP mRNA. Ideally, microinjection should introduce a pulse of exogenous RNA into a functioning endogenous pathway. The intracellular distribution of exogenous RNA should reflect that of endogenous RNA. Under the conditions used in this study, the distributions of exogenous and endogenous MBP mRNAs in the oligodendrocyte were qualitatively similar. However, the number of exogenous RNA granules in the microinjected cells (which reflects the amount of exogenous MBP mRNA) was generally greater than the number of endogenous RNA granules observed by in situ hybridization (which reflects the amount of endogenous MBP mRNA). These conditions were chosen to ensure that each intermediate in the pathway was populated with an amount of exogenous RNA sufficient to visualize.

Immediately after microinjection, exogenous RNA appears dispersed in the perikaryon. A small proportion of endogenous MBP mRNA in oligodendrocytes also appears dispersed in the perikaryon of intact cells. This represents the first intermediate in the proposed pathway. The dispersed

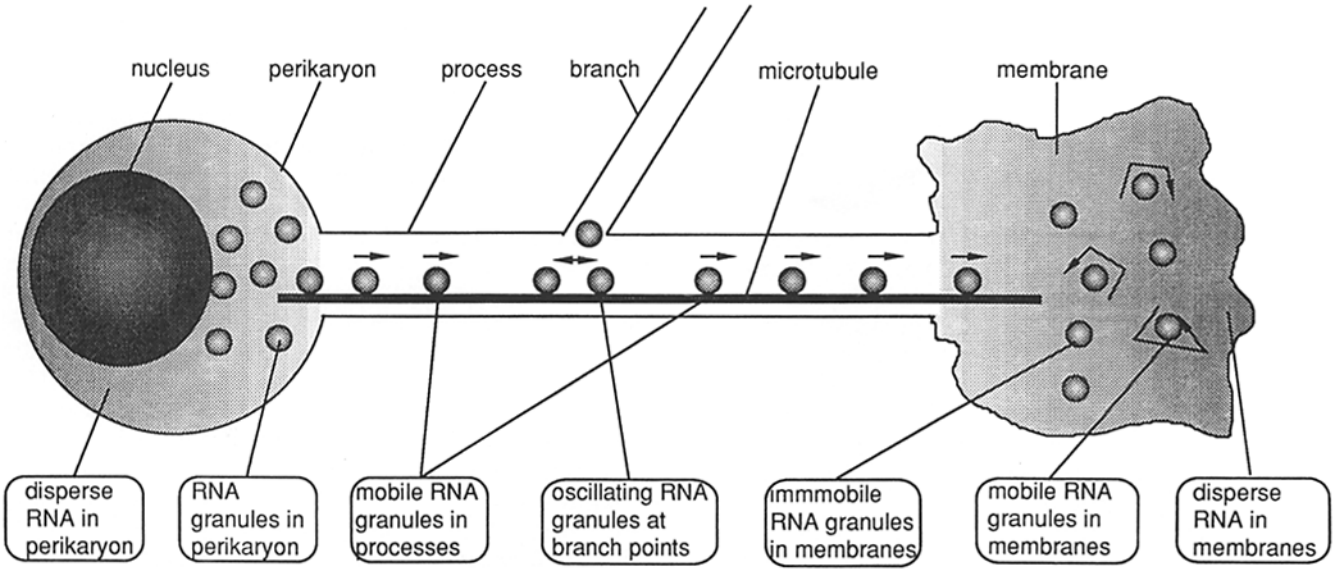

Figure 9. Multi-step model for transport and localization of MBP mRNA in oligodendrocytes. The diagram shows a schematic representation of an oligodendrocyte. Various subcellular compartments are indicated above the diagram. Postulated sequential intermediates in RNA transport and localization are indicated below the diagram. The diagram is not drawn to scale. The relative sizes of the granules and the microtubule within the cell are expanded for illustrative purposes.

RNA in the perikaryon is extracted with non-ionic detergent, indicating that it is not associated with the cytoskeletal matrix. This may represent MBP mRNA recently exported from the nucleus, before it associates with the cytoskeleton.

The dispersed exogenous RNA in the perikaryon is assembled into RNA granules within minutes of injection. Endogenous MBP mRNA in oligodendrocytes also appears as granules in the perikaryon. This represents the second intermediate in the proposed pathway. The RNA granules in the perikaryon are mobile. This was determined by direct epifluorescent microscopic observation but is not documented here because the density of granules in the perikaryon makes imaging and motion analysis of individual granules difficult. The mechanism for mobility of granules in the perikaryon is not known. The RNA granules in the perikaryon are not extracted with non-ionic detergent, indicating that they are associated with the cytoskeletal matrix. These results suggest that mRNA is assembled into cytoskeletal-associated granules within minutes of export from the nucleus.

The molecular mechanisms involved in RNA granule formation are unknown. In the case of exogenous RNA, granule formation occurs in the cytoplasm. RNA injected into the nucleus does not form granules and does not exit from the nucleus (data not shown). Several different mRNAs (MBP, globin, actin) were assembled into granules, but tRNA and dextran were not, indicating that granule formation is a general property of mRNAs. The structural features of mRNA that mediate granule formation are not known. Based on the fluorescence intensity, each granule contains several RNA molecules, but it is not known if a single granule contains multiple different mRNA species. Translation of mRNA is apparently not required for granule formation since digoxigenin-labeled RNA forms granules but is probably not translated because of the large number of substituted ribonucleotides.

This paper represents the first description of mRNA granules in cells. Other workers (Taneja et al., 1992), analyzing the intracellular distribution of poly A-containing RNA by in situ hybridization, have presented images showing a granular distribution of RNA in fibroblasts. However, individual granules were not resolved. This may be due to the thickness of the fibroblasts compared to oligodendrocytes, or because total poly A-containing RNA was visualized rather than a single species of mRNA. Also, the granular appearance of the RNA observed by previous workers may have been ascribed to fixation artifact. The RNA granules described here cannot be due to fixation because they are observed in live, unfixed cells.

Some MBP mRNA granules in the perikaryon appear to be aligned in tracks extending from the nucleus to the processes, with uniform spacing between individual granules. This was observed in both oligodendrocytes and neuroblastoma cells. The aligned granules are presumably associated with cytoskeletal elements (microfilaments or microtubules) traversing the cytoplasm. Alignment of MBP mRNA granules in tracks may represent an initial sorting mechanism that ultimately leads to differential transport and localization of MBP mRNA to the periphery of the oligodendrocyte. Non-MBP mRNA (globin and actin) granules were not aligned in tracks, indicating that this step may require specific *cis*-acting elements present in MBP mRNA. The spacing between individual granules in the tracks may reflect a rate-limiting step involved in association of MBP mRNA granules with the transport machinery.

MBP mRNA granules in the processes undergo sustained anterograde motion with a velocity of ~0.2 μm/s. This represents the third intermediate in the proposed pathway. The granules are aligned along microtubule bundles in the center of the processes. The sustained directional motion of mobile granules in processes suggests that this may represent a transport mechanism to translocate granules from the perikaryon to the periphery. The velocity of movement is consistent with microtubule-based, kinesin-driven transport (Okabe and Hirokawa, 1989; Vallee and Bloom, 1991).

At branch points in oligodendrocyte processes, sustained motion of MBP mRNA granules is sometimes interrupted and the granules undergo oscillatory motion with a mean displacement of ~0.1 μm/s. This represents the fourth intermediate in the proposed pathway. Clusters of RNA granules at branch points are observed with both endogenous and exogenous MBP mRNA and are associated with the cytoskeletal matrix, implying interaction with either microfilaments or microtubules. The basis for the oscillatory motion is not known. Mobile granules are observed distal to branch points, indicating that the interruption of motion is temporary. In many cases granules are found preferentially in one branch. This suggests that oscillatory interruption of motion and clustering of granules at branch points reflect a sorting mechanism to direct MBP mRNA transport to specific branch processes. If this step is rate limiting it could account for the clustering of granules at branch points. This mechanism could function in vivo to direct myelin formation around specific axons.

Many MBP mRNA granules are found in the flattened membrane sheets elaborated by oligodendrocytes. Some of these granules are relatively immobile, and some undergo random circulatory motion with a mean displacement of 1 μm/s. These represent the fifth and sixth intermediates, respectively, in the proposed pathway. The amplitude of displacement of the mobile granules suggests active movement rather than passive diffusion. The mechanism responsible for this motion is not known. It seems unlikely that the mobile granules in this region of the cell are translocating on microtubules, because the ordered distribution of microtubules would not support the random trajectories of granule motion that are observed. Since the granules are associated with the cytoskeletal matrix, it is possible that granule mobility in this region of the oligodendrocyte is mediated through microfilaments. The functional significance of the immobile and mobile MBP mRNA granules in the oligodendrocyte membrane sheets is not known. One hypothesis is that the immobile granules represent a stationary intermediate, after transport along microtubules has terminated, while the mobile granules represent a transitional intermediate between microtubule-associated transport and final dispersed localization in the membranes.

A proportion of MBP mRNA appears dispersed in the peripheral membrane sheets of oligodendrocytes in culture. This represents the seventh intermediate in the proposed pathway. There is a lag of several minutes before microinjected MBP mRNA appears dispersed in the membrane sheets, indicating that this may be the final destination of the RNA. The dispersed MBP mRNA is extracted with non-

ionic detergent, indicating that it is not associated with the cytoskeleton. The membrane sheets elaborated by oligodendrocytes in culture correspond to the myelin membrane which is wrapped around axons to form the myelin sheath in vivo. Localization of MBP mRNA to this region of the oligodendrocyte in culture is consistent with localization of MBP mRNA to the myelin sheath in vivo.

In summary, the results presented in this paper provide the basis for a coherent model describing the transport and localization of MBP mRNA in oligodendrocytes. One unexpected feature of this model is the involvement of RNA granules as intermediates in the pathway from the perikaryon to the peripheral membranes of the cell. To our knowledge, RNA granules of this type have not previously been described in cells. In addition, the differential intracellular localization of microinjected MBP mRNA compared to control mRNA provides a means of delineating the *cis*-acting elements in MBP mRNA that mediate its transport and localization in oligodendrocytes.

This work was supported by National Institutes of Health research grants to J. H. Carson (NS15190) and E. Barbarese (NS19943), an NIH Shared Instrumentation grant (RR03976), and a State of Connecticut Department of Higher Education Elias Howe grant.

Received for publication 9 February 1993 and in revised form 8 June 1993.

References

Barbarese, E. 1991. Spatial distribution of myelin basic protein mRNA and polypeptide in quaking oligodendrocytes in culture. *J. Neurosci. Res.* 29:271–281.

Berleth, T., M. Burri, G. Thoma, D. Bopp, S. Richstein, G. Frigerio, M. Noll, and C. Nusslein-Volhard. 1988. The role of localization of *bicoid* RNA in organizing the anterior pattern of the *Drosophila* embryo. *EMBO (Eur. Mol. Biol. Organ.) J.* 7:1749–1756.

Biegel, D., and J. S. Pachter. 1991. "In situ" translation: use of the cytoskeletal framework to direct cell-free protein synthesis. *In Vitro Cell. Dev. Biol.* 27A:75–85.

Bottenstein, J. E. 1986. Growth requirements in vitro of oligodendrocyte cell lines and neonatal rat brain oligodendrocytes. *Proc. Natl. Acad. Sci. USA.* 83:1955–1959.

Braun, R. E., J. J. Peschon, R. R. Behringer, R. L. Brinster, and R. D. Palmiter. 1989. Protamine 3'-untranslated sequences regulate temporal translational control and subcellular localization of growth hormone in spermatids of transgenic mice. *Genes & Dev.* 3:793–802.

Bruckenstein, D. A., P. J. Lein, D. Higgins, and R. T. Fremeau, Jr. 1990. Distinct spatial localization of specific mRNAs in cultured sympathetic neurons. *Neuron.* 5:809–819.

Burgin, K. E., M. N. Waxham, S. Rickling, S. A. Westgate, W. C. Mobley, and P. T. Kelly. 1990. In situ hybridization histochemistry of Ca^{2+}/calmodulin-dependent protein kinase in developing rat brain. *J. Neurosci.* 10: 1788–1798.

Colman, D. R., G. Kreibich, A. B. Frey, and D. D. Sabatini. 1982. Synthesis and incorporation of myelin polypeptides into CNS myelin. *J. Cell Biol.* 95:598–608.

Ephrussi, A. E., L. K. Dickinson, and R. Lehmann. 1991. *oskar* organizes the germ plasm and directs localization of the posterior determinant *nanos*. *Cell.* 66:37–50.

Feinberg, A. P., and B. Vogelstein. 1983. A technique for radiolabeling DNA restriction endonuclease fragments to high specific activity. *Anal. Biochem.* 132:6–13.

Fontaine, B., D. Sassoon, M. Buckingham, and J.-P. Changeux. 1988. Detection of the nicotinic acetylcholine *alpha*-subunit mRNA by in situ hybridization at neuromuscular junctions of 15-day-old chick striated muscles. *EMBO (Eur. Mol. Biol. Organ.) J.* 7:603–609.

Gergen, J. P., and B. A. Butler. 1988. Isolation of the *Drosophila* segmentation gene *runt* and analysis of its expression during embryogenesis. *Genes & Dev.* 2:1179–1193.

Giulian, D., B. Johnson, J. F. Krebs, M. J. Tapscott, and S. Honda. 1991. A growth factor from neuronal cell lines stimulates myelin protein synthesis in mammalian brain. *J. Neurosci.* 11:327–336.

Golumbeski, G. S., A. Bardsley, F. Tax, and R. E. Boswell. 1991. *tudor*, a posterior-group gene of *Drosophila melanogaster*, encodes a novel protein and an mRNA localized during mid-oogenesis. *Genes & Dev.* 5:2060–2070.

Holmes, E., G. Hermanson, R. Cole, and J. de Vellis. 1988. Developmental expression of glial-specific mRNAs in primary cultures of rat brain visualized by in situ hybridization. *J. Neurosci. Res.* 19:389–396.

Ingham, P. W., K. R. Howard, and D. Ish-Horowicz. 1985. Transcription pattern of the *Drosophila* segmentation gene *hairy*. *Nature (Lond.).* 318: 439–445.

Kachar, B., T. Behar, and M. Dubois-Dalcq. 1986. Cell shape and motility of oligodendrocytes cultured without neurons. *Cell Tissue Res.* 244:27–38.

Kimhi, Y., C. Palfrey, I. Spector, Y. Barak, and U. Z. Littauer. 1976. Maturation of neuroblastoma cells in the presence of dimethylsulfoxide. *Proc. Natl. Acad. Sci. USA.* 73:462–466.

Kim-Ha, J., J. L. Smith, and P. M. Macdonald. 1991. *oskar* is localized to the posterior pole of the Drosophila oocyte. *Cell.* 66:23–35.

Kleiman, R., G. Banker, and O. Steward. 1990. Differential subcellular localization of particular mRNAs in hippocampal neurons in culture. *Neuron.* 5:821–830.

Kristensson, K., K. V. Holmes, C. S. Duchala, N. K. Zeller, R. A. Lazzarini, and M. Dubois-Dalcq. 1986. Increased levels of myelin basic protein transcripts gene in virus-induced demyelination. *Nature (Lond.).* 322: 544–547.

Lawrence, J. B., and R. H. Singer. 1986. Intracellular localization of messenger RNAs for cytoskeletal proteins. *Cell.* 45:407–415.

Macdonald, P.M., P. Ingham, and G. Struhl. 1986. Isolation, structure, and expression of *even-skipped*: a second pair-rule gene of Drosophila containing a homeo box. *Cell.* 47:721–734.

Mohr, E., S. Fehr, and D. Richter. 1991. Axonal transport of neuropeptide encoding mRNAs within the hypothalamo-hypophyseal tract of rats. *EMBO (Eur. Mol. Biol. Organ.) J.* 10:2419–2424.

Morgan, F., E. Barbarese, and J. H. Carson. 1992. Visualizing cells in three dimensions using confocal microscopy, image reconstruction, and isosurface rendering: application to glial cells in mouse CNS. *Scanning Microsc.* 6:345–357.

Okabe, S., and N. Hirokawa. 1989. Axonal transport. *Curr. Opin. Cell Biol.* 1:91–97.

Pfeffer, S. R., and J. E. Rothman. 1987. Biosynthetic protein transportation and sorting by the endoplasmic reticulum and Golgi. *Annu. Rev. Biochem.* 56:829–852.

Rebagliati, M. R., D. L. Weeks, R. P. Harvey, and D. A. Melton. 1985. Identification and cloning of localized maternal RNAs from Xenopus eggs. *Cell.* 42:769–777.

Roach, A., K. Boylan, S. Horvath, S. B. Prusiner, and L. E. Hood. 1983. Characterization of cloned cDNA representing rat myelin basic protein: absence of expression in brain of shiverer mutant mice. *Cell.* 34:799–806.

Shiota, C., M. Miura, and K. Mikoshiba. 1989. Developmental profile and differential localization of mRNAs of myelin proteins (MBP and PLP) in oligodendrocytes in the brain and in culture. *Dev. Brain Res.* 45:83–94.

Singer, R. H., J. B. Lawrence, and C. Villnave. 1986. Optimization of in situ hybridization using isotopic and non-isotopic detection methods. *BioTechniques.* 4:230–251.

Singer, R. H., G. L. Langevin, and J. B. Lawrence. 1989. Ultrastructural visualization of cytoskeletal mRNAs and their associated proteins using double-label in situ hybridization. *J. Cell Biol.* 108:2343–2353.

Sundell, C. L., and R. H. Singer. 1991. Requirement of microfilaments in sorting of actin messenger RNA. *Science (Wash. DC).* 253:1275–1277.

Taneja, K. L., L. M. Lifshitz, F. S. Fay, and R. H. Singer. 1992. Poly(A) RNA codistribution with microfilaments: evaluation by in situ hybridization and quantitative digital imaging microscopy. *J. Cell Biol.* 119:1245–1260.

Vallee, R. B., and G. S. Bloom. 1991. Mechanisms of fast and slow axonal transport. *Annu. Rev. Neurosci.* 14:59–92.

Verity, N. A., and A. T. Campagnoni. 1988. Regional expression of myelin protein genes in the developing mouse brain: in situ hybridization studies. *J. Neurosci. Res.* 21:238–248.

Wang, C., and R. Lehmann. 1991. *Nanos* is the localized posterior determinant in Drosophila. *Cell.* 66:637–647.

Weir, M. P., and T. Kornberg. 1985. Patterns of *engrailed* and *fushi tarazu* transcripts reveal novel intermediate stages in *Drosophila* segmentation. *Nature (Lond.).* 318:433–439.

Wells, B. D., and C. R. Cantor. 1977. A strong ethidium binding site in the acceptor stem of most or all transfer RNAs. *Nucleic Acids Res.* 4(5): 1667–1680.

Wells, B. D., and C. R. Cantor. 1980. Ribosome binding by tRNAs with fluorescent labeled 3' termini. *Nucleic Acids Res.* 8(14):3229–3246.

Yisraeli, J. K., S. Sokol, and D. A. Melton. 1990. A two-step model for the localization of maternal mRNA in Xenopus oocytes. Involvement of microtubules and microfilaments in the translocation and anchoring of Vg1 mRNA. *Development.* 108:289–298.